Acta Chemica Scandinavica A 29 (1975) 489—498

Coordination and Bridge Formation in Molten Gallium(III)-Cesium Chloride Mixtures from Raman Spectroscopy

HARALD A. ØYE and WERNER BUES

Institute of Inorganic Chemistry, The Technical University of Norway, N-7034 Trondheim, Norway, and Institute of Inorganic Chemistry, The Technical University of Clausthal, Clausthal-Zellerfeld, German Federal Republic, D-3392

The Raman spectra of molten and solid mixtures of $GaCl_3$ and CsCl, as well as $CsAlGaCl_7$, have been investigated. The data are interpreted in terms of the successive formation of $GaCl_4^-$, $Ga_2Cl_7^-$, $Ga_nCl_{3n+1}^-$, $n \geq 3$, and Ga_2Cl_6 upon addition of $GaCl_3$ to CsCl. The data for $GaCl_4^-$ have been analyzed by the **FG** matrix method. Experimental evidence for strong bridge bonds in $Ga_2Cl_7^-$ and $Al_2Cl_7^-$ has been obtained. The frequencies of the aluminium and gallium chloride species are compared.

Although halogen bridges might be more common in inorganic chemistry than generally anticipated, few attempts have been made to characterize them. The present study of $GaCl_3-CsCl$ mixtures is part of a general study of chlorine bridges, which started with an investigation of molten $AlCl_3-KCl$.[1,2] This work has now been extended to include mixtures with LiCl and CsCl as well.[3] Bridge formations in $AlCl_3-MCl$ and $GaCl_3-MCl$ systems are accompanied by a very strong variation in acid-base characteristics, which make the mixtures suitable reaction media for inorganic as well as organic reactions.

In contrast to the $AlCl_3$-containing system, the present $GaCl_3$-CsCl system has the advantage of being completely miscible,[4] and a full study over the whole concentration range can be performed. The vibrational force constants of $GaCl_4^-$ are also rather similar to those of $AlCl_4^-$, as demonstrated by the close identity of frequencies for the two vibrational modes where the central atom is not moving.[2,5]

A brief account of some preliminary results on $GaCl_3-CsCl$ liquid mixtures has been published previously.[6]

EXPERIMENTAL

Apparatus. A Coderg PH 1 Raman spectrometer with a pulsed ruby laser, exciting line 6943 Å, was used. The time average power of the laser was between 500 and 150 mW, depending on the applied voltage and the operating time of the activating Philips 1000 W high pressure mercury pulse lamp. The detector was an EMI Electronics photomultiplier, type 9558 A. The Raman spectrometer apparatus is described in more detail by Bues, Brockner and Grünewald.[7] The partly circular and partly plane polarized ruby laser light is passed through a horizontal polarizer before reaching the sample. The 90° emitted Raman light is then passed through a horizontal polarizer (non-polarization spectra) or a vertical polarizer (polarization spectra), in front of the instrument's monochromator. The purpose of the horizontal polarizer in front of the monochromator for the non-polarization spectra was to reduce stray light.

Each sample was contained in a sealed cylindrical quartz cell, inner diameter 4 mm and length 20 mm, fitted with a side arm (Hellma, Müllheim Baden).[8] Independent experiments showed that the cells could withstand pressures up to 80 atm at 600 °C.

The optical cell (A) was contained in a stainless steel tube (B). These were both heated in a small furnace fitted to a Coderg multiple reflection Unit (M.R.) (Fig. 1). The scattered Raman light was observed through an opening in the furnace (C) perpendicular to the incident laser beam. On the opposite side of the Raman spectrophotometer was a mirror, which reflected the scattered light in this direction back to the spectrometer. The furnace was insulated with fire bricks (D) and water-cooled on the outside (E).

The temperature was controlled with four heating elements (F), two end elements, a middle element, and a top element. The two end elements were coupled in series. Each of

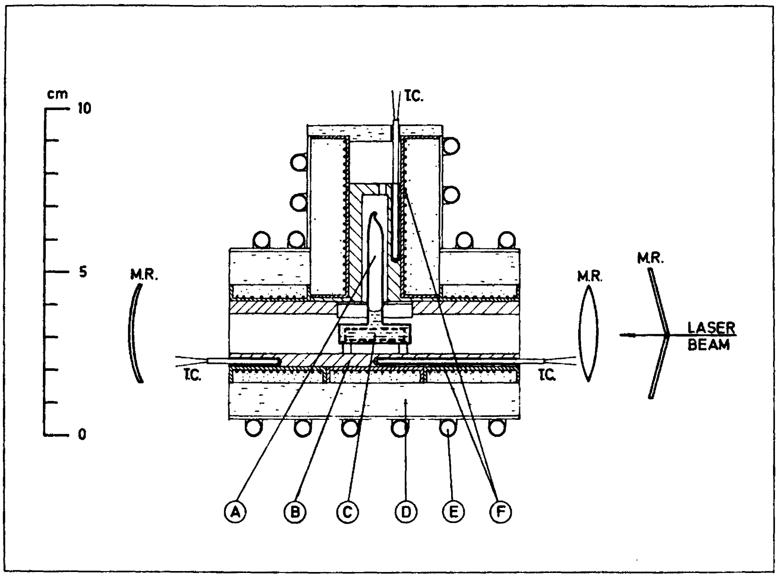

Fig. 1. Furnace with sample. A. Optical quartz cuvette with sample. B. Stainless steel tube. C. Opening for observation and back reflection. D. Fire bricks. E. Cooling coils. F. Kanthal heating wires. M. R. Coderg multiple reflection unit. T. C. Pt/Pt10Rh thermocouples.

the three heating circuits was regulated independently using a Pt/Pt10Rh thermocouple (T.C.) and proportional controllers, (PID+SCR, Eurotherm, Worthing, Sussex, England).

As the furnace had openings for the incident laser beam as well as for the scattered Raman light, temperature gradients in the sample were hard to avoid. To minimize cooling at the end windows, the end elements were kept 20°C above the middle element. Nevertheless, temperature gradients within the sample of $\pm 5°$ were observed by solidification experiments. Fortunately, the temperature was found not to be a sensitive parameter in the present investigation.

Chemicals. Anhydrous $GaCl_3$, 99,99 % was obtained in 10 g ampules from Schuchardt, München. Cesium chloride, *p.a.*, was obtained from Merck, Darmstadt. The CsCl was further purified by dissolution and re-crystallization in water and drying under vacuum at 400 °C. The salt was then melted and filtered through a quartz frit.

Procedure. In an N_2-filled glove-box (moisture content < 20 ppm) a calculated amount of $GaCl_3$ was transferred to a quartz tube above a quartz frit. The tube was evacuated to < 0.1 Torr and sealed off. (The poor vacuum was due to the relatively high vapour pressure of $GaCl_3$ at room temperature). The salt was then sublimed through the frit and condensed on the other side as large crystals. Small pieces of glass from the broken ampule remained on the frit. They were later weighed and their weight subtracted.

The optical cell was fused to a tube with a quartz frit. In the glove-box, a calculated amount of CsCl was added, together with the $GaCl_3$ and the tube connected to a vacuum-line and sealed.

The salts were melted and mixed in a Kanthal-wound quartz furnace. When the salts were thoroughly mixed, the temperature was suddenly raised and the furnace tilted. The sudden increase in vapour pressure pushed the melt through the frit and down into the optical cell. The optical cell was sealed off and was then ready for use.

RESULTS

The Raman spectra of liquid $GaCl_3-CsCl$ mixtures, retraced directly from the spectrometer charts, are shown in Figs. 2a and 2b, Fig. 2b giving polarization spectra for some selected compositions. See the experimental section for a description of the optical arrangement. The spectral slit width for the melt spectra was 8 cm^{-1} and the scanning rate was 30 cm^{-1}/min.

The given composition corresponds to the weighed-in amount of salt. Great care was

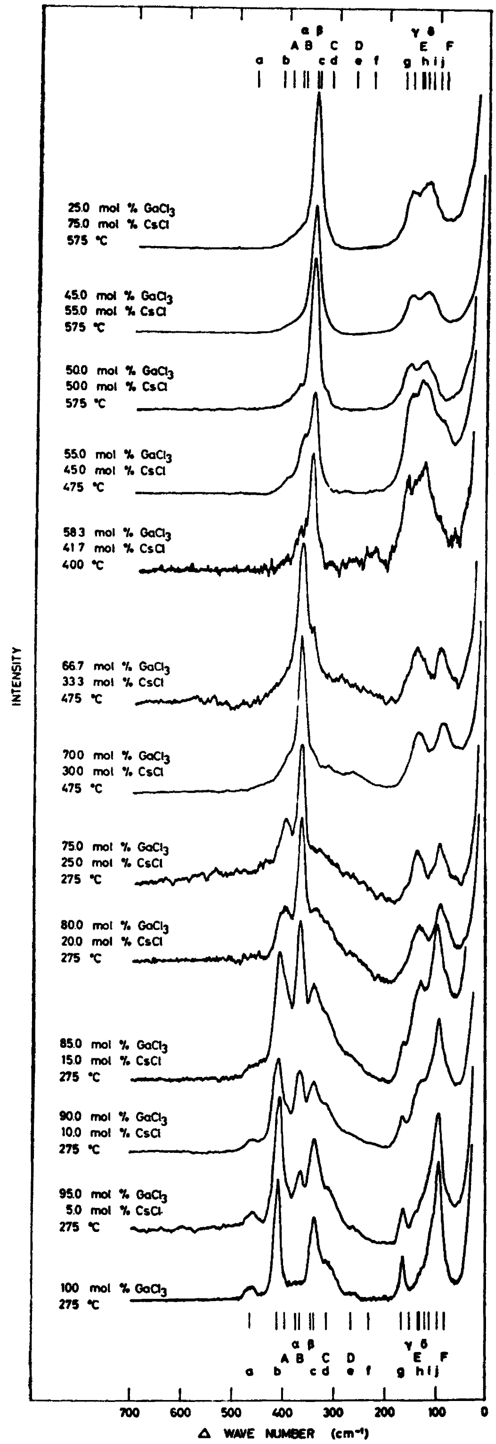

Fig. 2a. Raman spectra of liquid $GaCl_3-CsCl$ mixtures.

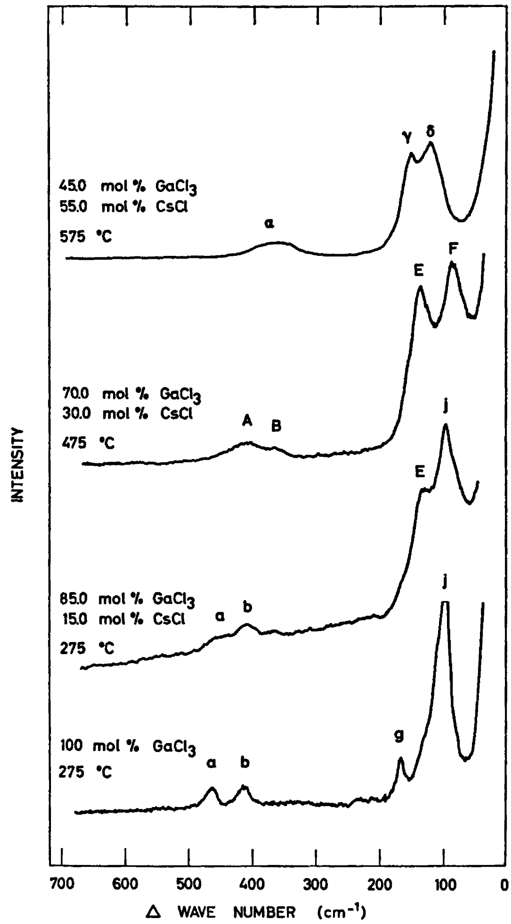

Fig. 2b. "Polarized" Raman spectra of some selected liquid mixtures of $GaCl_3-CsCl$.

taken to avoid evaporation losses, consequently no chemical analysis was performed after the experiments.

Because of the high vapour pressure of $GaCl_3$, it was not desirable to carry out the investigation isothermally. Fig. 2a gives the spectra as a function of composition in isothermal steps.

The Raman vibrational frequencies of molten $GaCl_3-CsCl$, solid $GaCl_3$ and solid $CsGaCl_4$ are listed in Table 1. Each value given is the average for all spectra recorded at the specific composition and temperature. The frequency was measured as the middle of the peak at 3/4 its maximum height. The standard deviation

Table 1. Raman vibration frequencies of molten $GaCl_3-CsCl$, solid $GaCl_3$ and solid $CsGaCl_4$ (cm^{-1}).[a]

$GaCl_4^-$				A	α	B(p)	β(p)	C	D		γ	E	δ			F	
$Ga_nCl_{3n+1}^-$, $n \leq 2$ Ga_2Cl_6		a	b(p)				c(p)	d(p)	e	f	g		h	i	j		k
Mol % $GaCl_3$	Temp. °C																
25.0	575				(374)		342				151		121				
45.0	575				(370)		343				153		120				
50.0	575				(375)		344				154		122				
55.0	475			(396)		(364)	344				(151)	(134)	(118)			(88)	
58.3	400					(367)	346				(153)	(137)	(125)			(90)	
66.7	475					365	(342)					136				89	
70.0	475			(393)		366	(344)	316	266			140				90	
75.0	275			394		365						135			(94)	(83)	
80.0	275			401		365	(335)	(306)	(262)		(166)	134			(94)	(80)	
85.0	275	(457)	409	(396)		367	338	(313)	(266)		(166)	133			97	(77)	
90.0	275	463	411	(392)		367	341	(313)	(266)		167	(136)			98	(78)	
95.0	275	464	411			368	342	(318)	267		168		(134)	(114)	98		
100.0	275	464	411				340	(320)	267	230	166		(130)	(110)	98		
$GaCl_3$(s)	30	457	406				(348)	329	243		167		125	115	102 98		43 35
$CsGaCl_4$(s)	35				(382)		354				157		126				

[a] Shoulders are given in parenthesis.

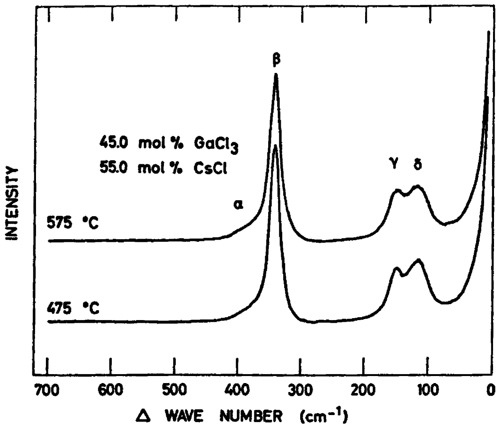

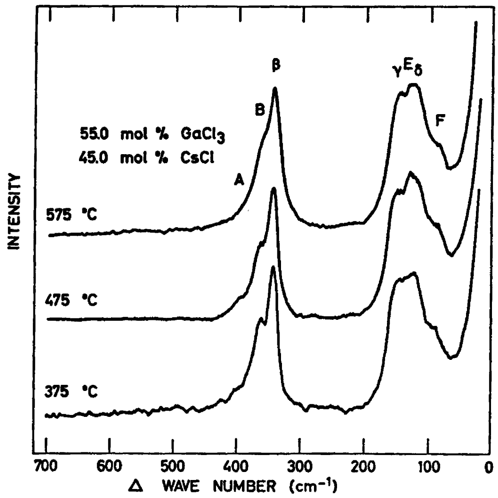

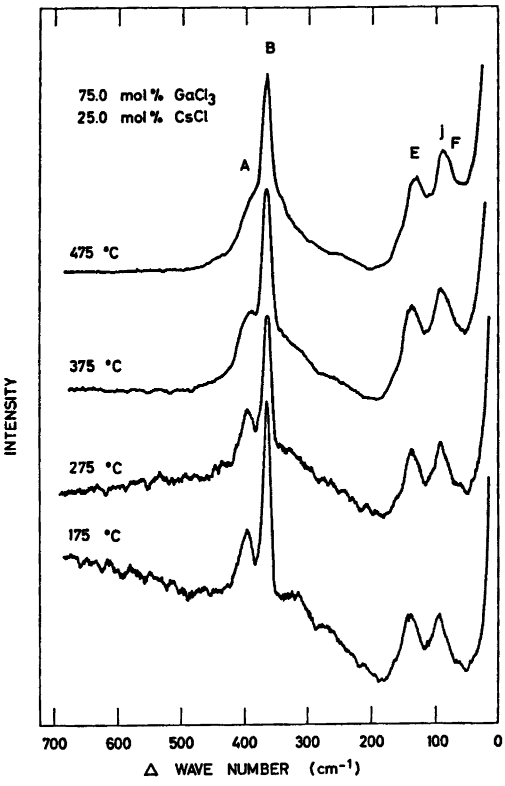

Fig. 3. Raman spectra of liquid $GaCl_3-CsCl$ mixtures as a function of temperature: (a) 45 mol % $GaCl_3$, (b) 55 mol % $GaCl_3$; (c) 75 mol % $GaCl_3$.

was ± 2 cm^{-1}. The recorder was calibrated using CCl_4. The polarization features of the bands are, in many cases, difficult to establish. Only peaks that are polarized with certainty are marked accordingly. Table 1 gives the assignment of the different lines to $GaCl_4^-$, $Ga_nCl_{3n+1}^-$, $n \geq 2$, and Ga_2Cl_6.

Figs. 3a, 3b and 3c demonstrate the influence of temperature on the Raman spectra of the liquid mixture $GaCl_3-CsCl$ at three compositions: (a) 45, (b) 55, and (c) 75 mol % $GaCl_3$.

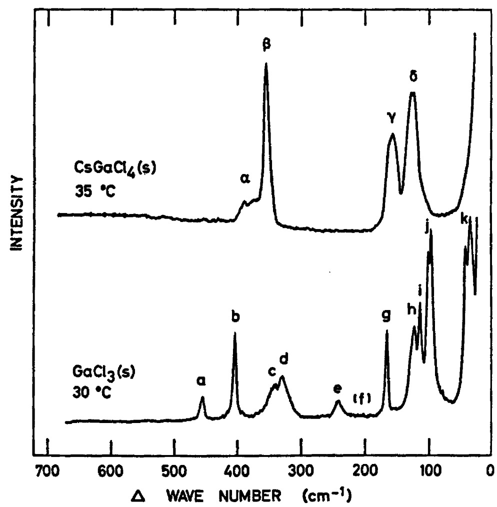

Fig. 4. Raman spectra of the solid compounds $CsGaCl_4$ and $GaCl_3$.

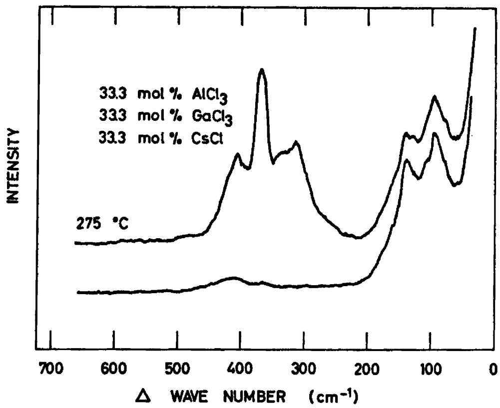

Fig. 5. Raman spectra of the liquid mixtures corresponding to the stoichiometry $CsAlGaCl_7$.

Fig. 4 gives the spectra of the solid compounds, $GsGaCl_4$ and $GaCl_3$. The latter was measured using a slit width of 2 cm^{-1}. Repeated attempts to obtain the spectra of the reported peritectic compound $CsGa_2Cl_7$[4] gave only background scattering and a featureless spectrum.

In order to obtain additional information about the bond structure in the Ga – Cl polymers, a spectrum of the mixture 33 mol % $GaCl_3$, 33 mol % $AlCl_3$ and 33 mol % CsCl was measured. This corresponds to the stoichiometry of $CsAlGaCl_7$. The results are given in Fig. 5.

DISCUSSION

Species formation. Upon inspection of Figs. 2a and 3a – c, it becomes apparent that the spectral contrasts between the different mixtures are not characterized by a gradual shift of the frequencies of the Raman bands. The spectral changes are, however, well described by Raman bands having definite frequencies. The relative intensities then change with composition and temperature. These indicate the presence of species equilibria in the melt mixtures, rather than gradual structural changes. The Raman frequencies in Table 1 have been interpreted accordingly.

The assignments have been performed as follows:

The spectral bands present in liquid mixtures with $X_{GaCl_3} \leq 0.50$, Fig. 2a, have been attributed to the tetrahedral $GaCl_4^-$ (Ref. 5) and marked $\alpha - \delta$. The relative intensities of these bands decrease with increasing $GaCl_3$ content above 50 mol % $GaCl_3$, corresponding to the stoichiometric composition of $CsGaCl_4$. The bands $\alpha - \delta$ correlate closely with the bands observed for the solid compound $CsGaCl_4$, Fig. 4.

The spectral bands in pure liquid $GaCl_3$, Fig. 2a, have been attributed to a double bridged Ga_2Cl_6, symmetry D_{2h}, and marked a – j. The relative peak intensities of these bands decrease with decreasing $GaCl_3$ content. The bands correspond closely to those of a previous investigation by Beattie and Horder,[8] and to those of solid $GaCl_3$ (Fig. 4), which is known to consist of Ga_2Cl_6 entities.[9]

Our spectrum of solid $GaCl_3$ agrees closely with that of Balls *et al.*[10] We obtained better resolution below 150 cm^{-1} which showed band splittings and new low-lying bands, probably caused by Ga_2Cl_6 rocking modes, (Table 1).

The bands not assigned to $GaCl_4^-$ or Ga_2Cl_6 have been attributed to polymers of the form $Ga_nCl_{3n+1}^-$, $n \geq 2$, and marked A – F.

Polymerization mechanisms. $Ga_2Cl_7^-$ in the form of two tetrahedra sharing one edge with a single chlorine bridge, is assumed to be one of the species present in the molten $GaCl_3$ – CsCl mixture. This is inferred from the similarity between the Raman spectroscopic bands assigned to $Al_2Cl_7^-$ and to $Ga_2Cl_7^-$,[6] and the presence of the solid compound $GsGa_2Cl_7$.[4] The double tetrahedron $Ga_2Cl_7^-$ also provides the natural structural link between the isolated $GaCl_4^-$ tetrahedrons for 50 mol % $GaCl_3$, and the Ga_2Cl_6 double-bridged tetrahedron for pure $GaCl_3$. Taylor has obtained the Raman spectra of solid Ga_3Cl_7 and KGa_2Cl_7.[11] Although the spectral details are somewhat different, the same strong band around 342 cm^{-1} is observed.

Species with a chlorine/gallium ratio lower than 3, for example $GaCl_2^+$, appear very unlikely in view of the strong chlorine affinity of gallium(III) chloride and the lack of evidence for dissociation of Ga_2Cl_6 into its monomers. An octahedral complex like $GaCl_6^{3-}$ can also be ruled out, since no Raman evidence for octahedral coordination is found at compositions corresponding to Cs_3GaCl_6, *i.e.* 25 mol % $GaCl_3$ (Fig. 2a). The radius ratio is also unfavourable for $GaCl_6^{3-}$.

Table 2. Integrated peak intensities in molten $GaCl_3-CsCl$ mixtures given in percentages of the band envelope between 250 and 800 cm^{-1} (from Fig. 2a).

Mol % $GaCl_3$	t °C	α	β	B	
25.0	575	13	87		
45.0	575	13	87		
50.0	575	13	79		
55.0	475	11	57	28	
58.3	475		59	21	
66.7	475	6	12	53	
70.0	475	15	9	50	
75.0	275	19		36	
80.0	275	19		36	
85.0	275	5	17	26	26
90.0	275	5	18	22	25
95.0	275		24	19	33
100.0	275		29		32
		A	c		b

The scattering of the Raman light is very sensitive to small changes in the experimental arrangement and the physical state of the sample. It is only with difficulty that the intensity of a Raman band can be used as a direct measure of species concentration. The relative intensities of the Raman bands for a certain species in the liquid state, however, are insensitive to changes in the environmental structure and temperature. This is demonstrated by $GaCl_4^-$ in the three upper curves in Fig. 2a and in Fig. 3a.

Table 2 lists the relative intensities of some of the more prominent Raman bands for the $GaCl_3-CsCl$ mixtures. The integrated peak intensities are determined from Fig. 2a as peak areas after dividing the total peak area between the different peaks, and are given as the percentage of the total peak intensity of the band envelope between 250 and 500 cm^{-1}. There is no established theoretical basis for this normalization, but the figures obtained by this method are more easily read than those found if only peak intensities, relative to other peak intensities, are tabulated. A fairly large margin of error must be allowed, due to the difficulties involved in separating overlapping peaks and subtracting the background scattering. The numbers in Table 2 may nevertheless have some physical meaning as demonstrated by the variation with increasing content of $GaCl_3$. A monotonic decrease in the peak assigned to $GaCl_4^-$ and an increase in the c and b peak assigned to Ga_2Cl_6, were observed. The most important feature of Table 2 is the relative variation of the band intensities of A and B. The intensity of A increases relative to B upon the addition of $GaCl_3$ beyond 66.7 mol % ($CsGa_2Cl_7$). A maximum around 75 mol % is observed, which corresponds to the stoichiometry of $CsGa_3Cl_{10}$. This is contrary to indications of the preliminary studies.[6] Hence $Ga_2Cl_7^-$ cannot be the only polymer present, but higher polymers, $Ga_nCl_{3n+1}^-$, $n \geq 3$, are formed.

The temperature variation of the Raman spectra supports also the assumption of the stepwise formation of $GaCl_4^-$, $Ga_2Cl_7^-$, Ga_nCl_{3n+1}, $n=3$, $n>3$? Fig. 3a, as previously mentioned, demonstrates the temperature insensitivity of the spectra for the mixture 45 mol % $GaCl_3-55$ mol % CsCl. Fig. 3b shows, for the mixture 55 mol % $GaCl_3-45$ mol % CsCl, that the peaks B and A, assigned to $Ga_2Cl_7^-$ and $Ga_nCl_{3n+1}^-$, $n \geq 3$, respectively, become less prominent with increasing temperature. Fig. 3c shows for the mixture 75 mol % $GaCl_3-25$ mol % CsCl that peak B increases relative to peak A with increasing temperature, *i.e.* the polymer $Ga_nCl_{3n+1}^-$, $n \geq 3$, becomes less prominent. This tendency toward a decrease in polymerization degree with increasing temperature is expected from statistical thermodynamic considerations.

The technique developed for calculating the equilibrium constant for the dissociation of $2Al_2Cl_7^- = 2AlCl_4^- + Al_2Cl_6$[2] can also be applied to this system. The species assumed to be present are $GaCl_4^-$, $Ga_2Cl_7^-$, $Ga_3Cl_{10}^-$ and Ga_2Cl_6. The many equilibrium data required and the difficulties in determining reliable relative intensities, however, make such a calculation impracticable and prone to uncontrollable errors. Our conclusions, therefore, are more qualitative in nature.

In the $GaCl_3-CsCl$ systems a stepwise formation of the species Ga_2Cl_6, $Ga_3Cl_{10}^-$ ($Ga_nCl_{3n+1}^-$, $n \geq 3$), $Ga_2Cl_7^-$, and $GaCl_4^-$ upon addition of CsCl to $GaCl_3$ is observed. A reasonable stoichiometric condition is that each species is at a maximum concentration at the corresponding bulk composition.

The corresponding composition as a function of the number of Ga atoms in the complex, n, is then given by $X_{GaCl_3} = n/(n+1)$. From Fig. 2 it can, however, be seen that $Ga_2Cl_7^-$ or $Ga_3Cl_{10}^-$ is not exclusively present at the respective mol fractions 0.67 and 0.75. Therefore, the equilibrium constants for the following dissociations are not negligible:

$$2Ga_2Cl_7^- = GaCl_4^- + Ga_3Cl_{10}^- \quad (1)$$

$$2Ga_3Cl_{10}^- = 2Ga_2Cl_7^- + Ga_2Cl_6 \quad (2)$$

The results found in the $GaCl_3-CsCl$ system closely parallel those recently found in $AlCl_3-CsCl$ mixtures.[3] In the $GaCl_3-CsCl$ system, however, there is only one band that can be assigned with certainty to higher polymers. In view of the general features of the Raman bands in Fig. 2, it is possible that the additional bands might be hidden, since despite the structural differences of $GaCl_4^-$, $Ga_2Cl_7^-$, and Ga_2Cl_6, the spectra have the same general features: A collection of bands containing the strongest polarizable peak is found between 380 and 450 cm^{-1}, and between 100 and 180 cm^{-1} another band envelope appears which contains the strongest depolarizable bands.

Gallium tetrachloride ion ($GaCl_4^-$). The observed Raman frequencies for $GaCl_4^-$ closely resemble those found by Woodward and Nord [5] for $GaCl_3$ dissolved in aqueous hydrochloric acid. The difference is less than 6 %.

For determining the vibrational force constants, the Wilson **FG**-matrix method is applied.[12] A modified valence force field and T_d symmetry are used,[13] setting non-diagonal **F**-matrix elements equal to zero.

$$F_{11}(A_1) = f_r + 3f_{rr}$$
$$F_{22}(E) = f_\alpha - 2f_{\alpha\alpha}$$
$$F_{33}(T_2) = f_r - f_{rr}$$
$$F_{44}(T_2) = f_\alpha$$

The calculation yields in mdyn/Å: $f_r = 1.842$, $f_{rr} = 0.210$, $f_\alpha = 0.147$, and $f_{\alpha\alpha} = 0.045$. The corresponding force constants (mdyn/Å) for $AlCl_4^-$ in $CsAlCl_4$ are: $f_r = 1.651$, $f_{rr} = 0.273$, $f_\alpha = 0.187$, and $f_{\alpha\alpha} = 0.044$.[3]

The close similarity in **F** matrix elements of $GaCl_4^-$ and $AlCl_4^-$ means that the difference in Ga–Cl and Al–Cl vibrations are mainly due to the mass difference between Al and Ga.

Digallium heptachloride ion ($Ga_2Cl_7^-$). The frequencies B, C, D, E, and F are assigned to $Ga_2Cl_7^-$. For the corresponding ion $Al_2Cl_7^-$ a double tetrahedral model with the sharing of one Cl and with symmetry D_{3d}[2] was previously assumed. The Al–Cl–Al bridge was assumed weak.[3]

The assumption of a weak bridge for $Al_2Cl_7^-$ was tested experimentally in the present work by obtaining the spectrum of $CsAlGaCl_7$ (Fig. 5) and comparing it with the spectra of $CsAl_2Cl_7$ and $CsGa_2Cl_7$. If the bridge force constant is very weak, the bridge would act as a vibrational insulator and the spectra of $AlGaCl_7^-$ should be superimposed on the spectra of $Al_2Cl_7^-$ and $Ga_2Cl_7^-$. This is not the case. In addition to the strong peaks at 311 and 366 cm^{-1}, corresponding to the strongest peaks for $Al_2Cl_7^-$ and Ga_2Cl_7, a strong polarizable peak at 405 cm^{-1} is observed, rendering a weak bridge model highly unlikely.

Recent structural work on crystals of $Pd_2(Al_2Cl_7)_2(C_6H_6)_2$,[14] $Te_4(Al_2Cl_7)_2$,[15] as well as KAl_2Br_7,[16] all give a bent Al–X–Al bridge (X = Cl, Br), the angle being close to the tetrahedral angle and the bridge bond length being only slightly larger than the terminal Al–X bond length.

The Raman spectrum of $CsAlGaCl_7$, the apparent stability of $Ga_2Cl_7^-$ and $Al_2Cl_7^-$, as well as the similarities in bond length between the Al–X bridge and the terminal Al–X in solid crystals, all point to a strong bridge force constant in the $Al_2Cl_7^-$ and $Ga_2Cl_7^-$ ions.

The bent Al–XI–Al bridge found in solid crystals does not necessarily imply a bent bridge for $Al_2Cl_7^-$ and $Ga_2Cl_7^-$ in liquid mixtures. In spite of the good quality Raman-spectra of the $GaCl_3-CsCl$ liquid mixtures, no more than 5 Raman active frequencies have been detected, compared with a minimum of 21 expected for a bent bridge. A calculation based on a D_{3d} model, not given here, also gives a reasonable explanation of the spectra.

Nevertheless, a bent bridge structure in the melt with, for instance, C_{2v} symmetry cannot be excluded, as it may give the same general spectrum as a D_{3d} model, having two major band envelopes around 350 and 100 cm^{-1}, the fine structure being blurred by thermal movements. As a conclusion we will, however,

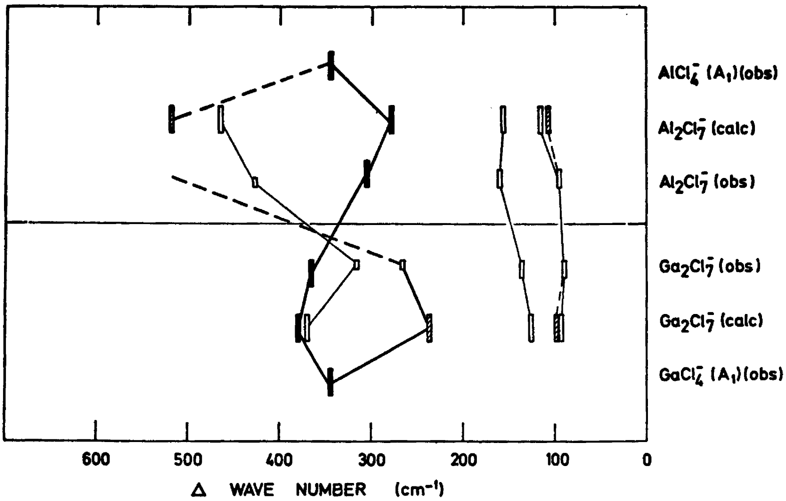

Fig. 6. Correlation diagram. Diagram illustrating the connection between calculated and observed Raman-active frequencies for $Al_2Cl_7^-$ and $Ga_2Cl_7^-$, D_{3d} and the "cross over" of $Al_2Cl_7^-$ and $Ga_2Cl_7^-$ modes. A strong chlorine bridge is assumed. Filled columns: Vibrational modes involving stretching of r. Hatched columns: Other total symmetric modes.

emphasize that the present melt studies do not give any positive evidence for such a structure.

A correlation diagram for observed frequencies for $Al_2Cl_7^-$ and $Ga_2Cl_7^-$ is given in Fig. 6. The valence stretch frequencies for $AlCl_4^-$ and $GaCl_4^-$ are also shown. In the present correlation diagram frequencies with similar vibrational characteristics have been joined together, and differs somewhat from the diagram given in the preliminary publication.[6]

The symmetric stretching frequencies of $AlCl_4^-$ and $GaCl_4^-$ are independent of the mass of the central ion, and are found to be approximately equal. In view of this fact, it might seem surprising that the strongest polarized frequency of $Ga_2Cl_7^-$ is at a higher frequency than for $Al_2Cl_7^-$, as a mass effect would predict the opposite trend.

This is considered due to the fact that the mass of Cl is intermediate between Al and Ga. The valence stretch frequency of $MeCl_4^-$ can for $Me_2Cl_7^-$ be considered split up in an end and bridge frequency, and a "cross over" is obtained when going from $Al_2Cl_7^-$ to $Ga_2Cl_7^-$.

This "cross over" for $Me_2Cl_7^-$ can be explained qualitatively from a **GF** matrix calculation where for simplicity a D_{3d} model was chosen. Assuming a bridge stretch force constant being 90 % of the terminal force constant and assigning the different vibrational modes according to the potential energy distribution,[17,18] the observed shifts in the A_g stretching modes for $Al_2Cl_7^-$ relative to $Ga_2Cl_7^-$ were reproduced. A parallel phenomenon is described by Sicbert [19] for XCN molecules. For X being very much lighter or very much heavier than C the CN frequency was about the same. For intermediate masses of X the CN frequency was shifted to lower frequencies for X lighter than N, and to higher frequencies for X heavier than N, with a similar "cross-over".

Acknowledgement. We gratefully acknowledge grants for instruments and materials from Volkswagenstiftung and experimental assistance from Mr. D. Grünewald and Mr. M. Sørlie. We appreciate the use of the computer programs of Dr. S. J. Cyvin. H. A. Ø. is thankful for support from Norges almenvitenskapelige forskningsråd.

REFERENCES

1. Cyvin, S. J., Klæboe, P., Rytter, E. and Øye, H. A. *J. Chem. Phys. 52* (1970) 2776.
2. Øye, H. A., Rytter, E., Klæboe, P. and Cyvin, S. J. *Acta Chem. Scand. 25* (1971) 559.

3. Rytter, E., Øye, H. A., Cyvin, S. J., Cyvin, B. N. and Klæboe, P. *J. Inorg. Nucl. Chem. 35* (1973) 1185.
4. Fedorov, P. J. and Tsimbalist, V. V. *Russ. J. Inorg. Chem. 9* (1964) 908.
5. Woodward, L. A. and Nord, A. A. *J. Chem. Soc.* (1965) 3721.
6. Øye, H. A. and Bues, W. *Inorg. Nucl. Chem. Lett. 8* (1972) 31.
7. Bues, W., Brockner, W. and Grünewald, D. *Spectrochim. Acta A 28* (1972) 1519.
8. Beattie, I. R. and Horder, J. R. *J. Chem. Soc. A* (1969) 2655.
9. Wallwork, S. C. and Worral, I. J. *J. Chem. Soc.* (1965) 1816.
10. Balls, A., Downs, A. J., Greenwood, N. N. and Straughan, B. P. *Trans. Faraday Soc. 62* (1966) 521.
11. Taylor, M. J. *J. Chem. Soc. A* (1970) 2812.
12. Wilson, E. B., Decius, J. C. and Cross, P. C. *Molecular Vibrations*, McGraw Hill, New York 1955.
13. Cyvin, S. J. *Molecular Vibrations and Mean Square Amplitude*, Universitetsforlaget, Oslo 1968, p. 121.
14. Allegra, G., Casogrande, G. T., Immirzi, A., Porri, L. and Vitulli, G. *J. Amer. Chem. Soc. 92* (1970) 289.
15. Cough, T. W., Lokken, D. A. and Corbett, J. D. *Inorg. Chem. 11* (1972) 357.
16. Rytter, E., Rytter, B. E. D., Øye, H. A. and Krogh-Moe, J. *Acta Crystallogr. B 29* (1973) 1541.
17. Morino, Y. and Kuchitsu, K. *J. Chem. Phys. 20* (1952) 1809.
18. Nakamoto, K. *Infrared Spectra of Inorganic and Coordination Compounds*, 2nd Ed., Wiley, New York 1970, p. 68.
19. Siebert, H. *Anwendungen der Schwingungsspektroskopie in der Anorganische Chemie*, Springer, Berlin 1966, p. 11.

Received December 13, 1974.